The Meteoritical Society

*Meteoritics & Planetary Science* 45, Nr 3, 383–393 (2010)
doi: 10.1111/j.1945-5100.2010.01029.x

# The Berduc L6 chondrite fall: Meteorite characterization, trajectory, and orbital elements

Josep M. TRIGO-RODRÍGUEZ[1,2*], Jordi LLORCA[3], José M. MADIEDO[4], Gonzalo TANCREDI[5], Wayne N. EDWARDS[6], Alan E. RUBIN[7], and Patrick WEBER[8]

[1]Institute of Space Sciences-CSIC, Campus UAB, Facultat de Ciències, Torre C5-parell, 2a, 08193 Bellaterra, Spain
[2]Institut d'Estudis Espacials de Catalunya, Gran Capità 2-4, Ed. Nexus, 08034 Barcelona, Spain
[3]Institut de Tècniques Energètiques, Universitat Politècnica de Catalunya, Diagonal 647, 08028 Barcelona, Spain
[4]Facultad de Ciencias Experimentales. Universidad de Huelva, 21071 Huelva, Spain
[5]Departamento de Astronomía, Facultad de Ciencias (DAFC), Iguá 4225, 11400 Montevideo, Uruguay
[6]Natural Resources Canada, Atlantic and Western Canada Branch, Canadian Hazards and Information Service, Earth Sciences Sector, 7 Observatory Crescent, Ottawa, Ontario, Canada K1A 0Y3
[7]Institute of Geophysics and Planetary Physics, University of California Los Angeles (UCLA), Los Angeles, California 90095–1567, USA
[8]Laboratory for High Energy Physics, University of Bern, Sidlerstrasse 5, CH-3012 Bern, Switzerland
[*]Corresponding author. E-mail: trigo@ieec.uab.es

*(Received 14 July 2009; revision accepted 11 December 2009)*

**Abstract**–The fall of the Berduc meteorite took place on April 7, 2008, at 01 h 02 min 28 s ± 1 s UTC. A daylight fireball was witnessed by hundreds of people from Argentina and Uruguay, and also recorded by an infrasound array in Paraguay. From the available data, the fireball trajectory and radiant have been reconstructed with moderate accuracy. The modeled trajectory was tested to fit the infrasound and strewn field data. From the computed apparent radiant $\alpha = 87 \pm 2°$ and $\delta = -11 \pm 2°$ and taking into account a range of plausible initial velocities, we obtained a range of orbital solutions. All of them suggest that the progenitor meteoroid originated from the main asteroid belt and followed an orbit of low inclination. Based on petrography, mineral chemistry, magnetic susceptibility, and bulk chemistry, the Berduc meteorite is classified as an L6 ordinary chondrite.

## INTRODUCTION

A bolide much brighter than the full Moon was widely seen over Argentina and Uruguay on April 7, 2008 at 01 h 02 min 28 s ± 1 s UTC. The event was magnificent; its absolute magnitude was indirectly inferred from daylight sensors placed in a nearby location to the main flare. An eyewitness from Ruteri Ruta (Argentina, Long. 58.123°W, Lat. 31.445°S) reported that due to the light emitted during the fireball's flare, the street lights were turned off automatically. Some estimations of the sensitivity of this automatic system suggest that the absolute magnitude of the main flare was probably in the −16 ± 3 range. The fireball's entrance also produced low frequency sound waves that were recorded by an infrasound array (station I41PY). Eyewitnesses, interviewed by Gonzalo Tancredi and Leda Sánchez (Departamento de Astronomía Facultad de Ciencias, Montevideo, Uruguay; DAFC), reported that the fireball traveled from the west to the east and experienced several fragmentations along its trajectory causing audible detonations that shattered windows in the area of the fall. Several stones were found by members of the Asociación Entrerriana de Astronomía (AEA) a few days after the fall in the countryside around Colonia Berduc. The largest piece in a public institution is a 154 g sample located in Museo de Ciencias Naturales y Antropológicas "Prof. Antonio Serrano" (MNCNA-AS) that acts as the hosting institution. The museum La Estación de Ubajay (MLEDU-Argentina) has a 95 g piece, and Complejo Astronómico El Leoncito

Fig. 1. The largest recovered Berduc sample weighing 5.53 kg. Images courtesy of O. A. Turone.

(CASLEO-Argentina) has a piece of 21 g. The rest of the mass remaining in Argentina is in private collections.

AEA members contacted the Spanish Meteor and Fireball Network (SPMN) after the fall to receive instructions on how to instigate a search for meteorites. AEA members found the first meteorites on April 8, and alerted the public media. These first pieces were found at coordinates longitude 58°19′45″W and latitude 31°54′39″S. A couple of these pristine samples, quickly recovered from the ground, were analyzed by our team. Several meteorite dealers alerted by the news also contributed to the recovery of additional pieces, but the samples were sold around the world. Most of the pieces remaining in Argentina were collected in the first few days after the fall and were unaffected by the weather. Tancredi and his group (DAFC) visited the zone 2 weeks after the fall and made a wide survey of the area. No additional meteorites were found close to the original finds. In total, about 10 meteorite samples were found to our knowledge, the total recovered mass being about 737 g (Connolly 2009). Óscar A. Turone informed us that a 5.5 kg piece at the front of the strewn field was recovered by local residents near Quebracho (Uruguay), but its exact fall location remains unclear as we discuss below. Unfortunately, this extraordinary sample was quickly sold to dealers, but was first photographed by Turone (see e.g., Fig. 1). A field search performed in the area by Turone concluded with the recovery of a 6 g complete stone that, after being thin-sectioned for careful study, proved to be a member of the Berduc fall. The first thin sections were made in Barcelona, Spain, in June 2008.

Most of the specimens found were quickly identified as meteorites because they exhibited a prominent fusion crust covering part of their surface, and were attracted by a magnet (Fig. 1). The interior of those pieces that broke during impact appears granular and dominated by large chondrules. Most of the large pieces were broken, but the small ones exhibit a complete fusion crust.

## TRAJECTORY, RADIANT, AND RANGE OF ORBITS

DAFC members interviewed over 30 eyewitnesses in Uruguay and Argentina, obtaining a reasonable number of theodolite measurements (see Table 1). After a careful study of the data, consistent reports were obtained from six locations. A compromise among the different stations was obtained and tested by using the available infrasound and strewn field data. The data treatment was similar to that of recent studies of other

Table 1. Visual eyewitnesses interviewed to estimate Berduc's bolide trajectory whose data have been considered in the present determination of the fireball trajectory and radiant.

| Site | Longitude W (°) | Latitude (°) | Beginning Az, Alt (°) | End Az, Alt (°) | Duration (s) |
|---|---|---|---|---|---|
| Fray Bentos | 58.3154 | −33.1123 | 295, 22 | 301, 18 | – |
| Chapicuy | 57.8893 | −31.6616 | 314, 25 | 229, 13 | 2 |
| Dayman termas | 57.9084 | −31.5327 | 353, 36 | 240, 21 | 2 |
| San Salvador (Argentina) | 58.5136 | −31.6279 | 249, 65 | 163, 85 | 5 |
| Camino Rusi-La Paz | 56.2111 | −34.7554 | 312, 8 | 326, 0 | 5–6 |
| Paraná | 60.5242 | −31.7359 | 120, 30 | 120, 18 | – |

bolides (Docobo et al. 2008; Trigo-Rodríguez et al. 2009). This time new software was written that specifically allowed us to define the observing locations that yielded consistent trajectories with the infrasound data. From the theodolite measurements obtained from the consistent locations, we determined an average trajectory employing the method of intersecting planes (Ceplecha 1987).

The position of the different locations was geometrically favorable for determining the fireball trajectory with moderate accuracy. Nine observers from six locations (Table 1) provided the most consistent data on the apparent path and duration of the bolide. The position of the meteorite strewn field was also used, but the drift caused by winds during the meteorite's dark flight was not taken into account. Upper air winds at the time were generally light and westerly below 20 km altitude in the area of the fall, according to UKMO meteorological data (Swinbank and O'Neill 1994; see Fig. 2), and significant rotation of the strewn field due to wind drift is not predicted from darkflight calculations (Ceplecha 1987). The fireball's trajectory projected on the ground is shown in Fig. 3. The coordinates of the bolide's beginning and ending points are given in Table 2. According to the finders, the 5.5 kg meteorite shown in Fig. 1 was found near Quebracho (Uruguay) about 25 km east from Colonia Berduc (see Fig. 3). We note that such a location is aligned with the computed trajectory, and we thought initially would fit with a fragmentation at a height of 20 km or higher. Despite this, when we ran the darkflight for a 5.5 kg test particle released from the fireball end at an usual velocity of about 4 km $s^{-1}$, we noticed that it does not cross the Argentina/Uruguay border. The computed landing point would be to the east of the town of Ubajay, but not having the exact fall coordinates for the 5.5 kg piece we remain skeptical on its exact country of recovery. It is important to remark that there is no regulation in Uruguay regarding the ownership and commerce of meteorites, as opposed to that in Argentina where the commerce is forbidden by law. It could be of concern in bordering cases like this. Several DAFC expeditions to the Quebracho area a couple of months after the fall were unable to find additional pieces or reports from local residents.

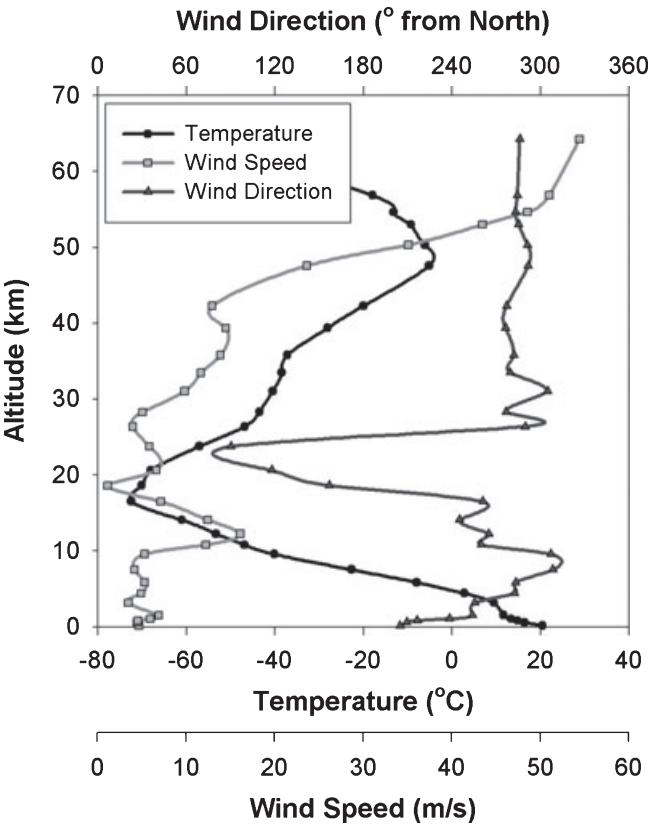


Fig. 2. U.K. Met Office vertical profile of the atmospheric temperature and wind field on April 7, 2008, taken near the end point of the observed fireball.

Table 2. Computed trajectory of the bolide projected on the ground.

| Beginning point ($h$ = 89.8 km) | | Ending point ($h$ = 18.3 km) | |
|---|---|---|---|
| Longitude (°) | Latitude (°) | Longitude (°) | Latitude (°) |
| 60.043 W | −31.568 | 58.432 W | −31.785 |

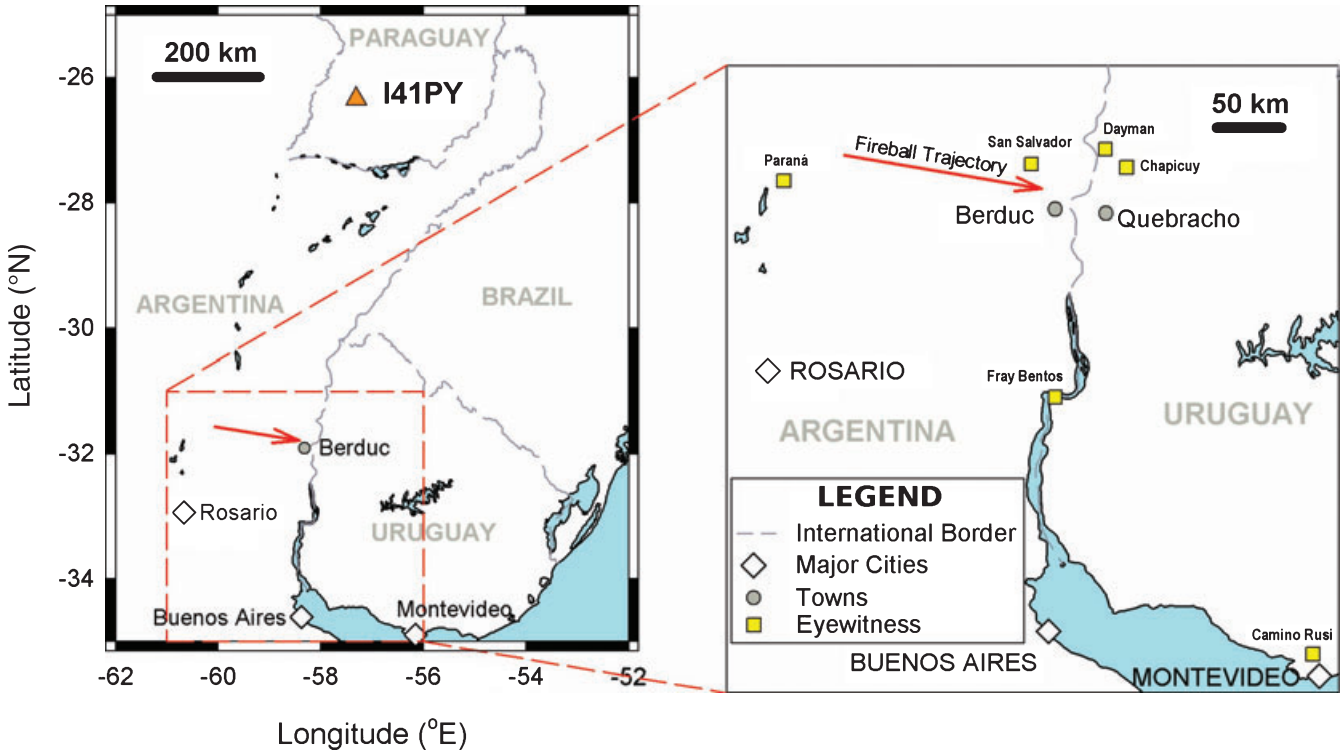


Fig. 3. Regional map of the Berduc meteorite fall. Inset: eyewitness locations in relation to the computed trajectory of Berduc bolide (arrow) showing the location of the recovered meteorites and the country borders. For more details, see the text.

Table 3. The estimated radiant coordinates and trajectory beginnings (for the fixed beginning height of 65 km).

| Apparent radiant | | | | Beginning point ($h$ = 89.8 km) | |
|---|---|---|---|---|---|
| Azimuth (°) | Elevation (°) | α (°) | δ (°) | Longitude (°) | Latitude (°) |
| 274 | 28.2 | 87 ± 2 | −11 ± 2 | 60.043 W | −31.568 |

The azimuth is measured from the north toward the east.

From the computed trajectory, we were able to obtain the apparent radiant of the bolide (Table 3). The duration of the bolide was reported by 18 eyewitnesses, being in the range of 3–6 s. From the trajectory length measured from some of the stations, we were unable to deduce a precise velocity, but we fixed an upper limit of 16 km $s^{-1}$. In this regard, Camino Rusi, Chapicuy, Dayman, and San Salvador reports were particularly relevant (Table 1). Eyewitnesses from Camino Rusi and San Salvador probably observed the full bolide, reporting a duration of 5 or 6 s. Observers from Chapicuy and Dayman observed the terminal part of the bolide path, and consequently reported a duration of about 2–3 s. In fact, an initial velocity higher than this is unlikely on dynamic grounds as we discuss below. Consequently, assuming a reasonable range of pre-atmospheric velocities (12–16 km $s^{-1}$), the possible orbital elements for the progenitor meteoroid were computed (Table 4). Almost all the orbital solutions suggest a low-inclination, medium-eccentricity orbit with an origin in the main asteroid belt; this is similar to the nine previously reported meteorite falls where accurate determinations of the orbital elements were made (e.g., Trigo-Rodríguez et al. 2006).

## INFRASOUND DATA

Infrasound data were obtained from IMS station I41PY at a great circle range of 614 km from the computed fireball end point (Fig. 4), and measurements are compiled in Table 5. Unfortunately, only two of the four microbarograph sensors were operational at the station on this date, so the signal association based on back-azimuths alone cannot be absolutely made (the solutions are degenerate). If, however, an apparent horizontal velocity of 350 m $s^{-1}$ is assumed for the

Table 4. Tentative orbital elements (J2000.0) for the probable range of radiant azimuths and several possible pre-atmospheric velocities of the fireball.

| Velocity (km $s^{-1}$) | $a$ (AU) | $e$ | $q$ (AU) | $Q$ (AU) | ω (°) | Ω (°) | $i$ (°) |
|---|---|---|---|---|---|---|---|
| 12 | 1.38 | 0.30 | 0.965 | 1.80 | 328 | 197.475 | 2.9 |
| 14 | 2.18 | 0.55 | 0.970 | 3.39 | 336 | 197.479 | 6.1 |
| 16 | 4.3 | 0.78 | 0.973 | 7.69 | 339 | 197.481 | 8.4 |
| Summary | >1 | Any | 0.969 ± 0.004 | >1 | 334 ± 6 | 197.478 ± 0.003 | <9 |

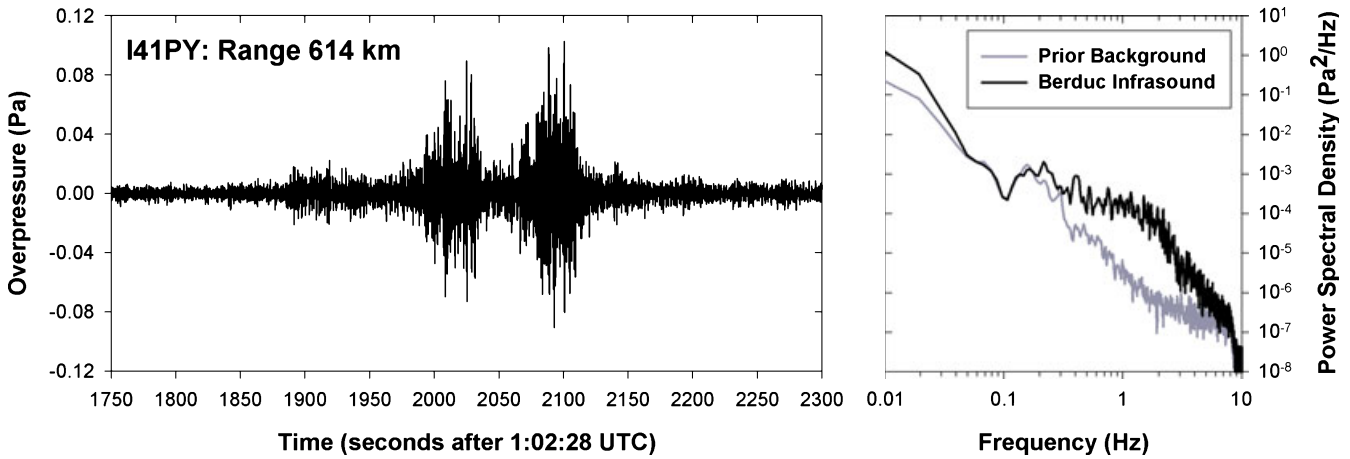


Fig. 4. Observed infrasound signals related with the entry of the Berduc fireball at I41PY in Villa Florida, Paraguay, and its associated power spectrum. Signal comprises three distinct phases likely originating from a source region near the end of the visible fireball between 30 and 18 km altitude. Waveform represents the array's "best beam," an average station waveform with channels stacked assuming a back azimuth of 188.3°, and has been highpass filtered at 0.5 Hz. Spectral density of the signal is shown relative to the spectral content of ambient noise of the same duration recorded just prior to the signal's onset.

Table 5. Berduc infrasound signal properties as recorded from station I41PY.

| I41PY—Villa Florida Array (26.342°S, 57.312°W, 0.164 m.a.s.l.) | |
|---|---|
| Hilbert amplitude (Pa) | 0.106 ± 0.022 |
| Peak to peak amplitude (Pa) | 0.183 ± 0.026 |
| Prior RMS noise (Pa) | 0.0030 ± 0.0019 |
| Post RMS noise (Pa) | 0.0024 ± 0.0014 |
| Period at maximum amplitude (s) | 1.85 ± 0.53 |
| Peak frequency (Hz) | 0.54 ± 0.15 |
| Signal to noise ratio | 18.8 ± 4.8 |

The Hilbert amplitude is the maximum amplitude of the signal envelope computed from the Hilbert transform of the signal (for more details on these measurements, see Edwards et al. 2006).

signal propagating across the array (typical of a grazing incidence for stratospheric arrivals), the observed time delay between the two operational sensors is well matched with back azimuths between 185.3° and 188.3° (measured eastward from the north). This is consistent with an event near the Argentina-Uruguay border and with an origin near the end point of the fireball's computed trajectory (a back azimuth of 189.9°). Subsequent acoustic ray tracing from the known fireball path to I41PY reproduces only the arrival of the third pulse seen in Fig. 5, by the arrival of a number of potential stratospheric paths originating from the lowest region of the trajectory between 18 and 30 km altitude. Again this is consistent with the time of the fireball and results in a 0.31 km $s^{-1}$ mean signal speed typical of stratospheric arrivals (Edwards et al. 2006). The remaining two earlier phases as yet remain unidentified, although these may represent faster propagating tropospheric phases based on the relative times of arrival and observations of previous fireballs (e.g., Arrowsmith et al. 2007). Limitations in available meteorological data in this region at the time of the fireball, unfortunately, do not allow us to explore this hypothesis further.

An analysis of the recorded infrasound signals in period and amplitude (Table 5), following the procedures of Edwards et al. (2006), suggests that the fireball had a kinetic energy of 0.025 ± 0.014 kt of equivalent TNT, similar to that of Villalbeto de la Peña (Llorca et al. 2005). One kiloton of TNT (1 kt) is equivalent to $4.185 \times 10^{12}$ Joules. As the source region for the observed signal is interpreted to have originated near the end of the visible fireball, potentially from the

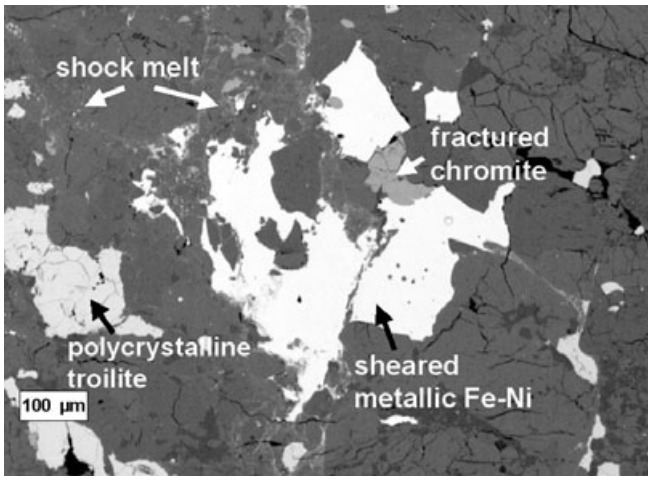


Fig. 5. Region of Berduc showing various shock features including polycrystalline troilite, sheared metallic Fe-Ni, fractured chromite, and a fine-grained shock melt transecting silicate grains.

significant fragmentations reported by eyewitnesses, this inferred kinetic energy can be viewed as a lower limit as it may represent the energy of the body only near the end of its atmospheric entry. From this energy evaluation, assuming a spherical body, coupled with the range of probable velocities and the meteorite's stony nature, we estimate that the Berduc meteoroid's pre-atmospheric size was roughly 1 m in diameter (Brown et al. 2002).

## MINERALOGY, PETROGRAPHY, AND CLASSIFICATION

A thin section UCLA 1900 of Berduc was examined microscopically in transmitted and reflected light. Grain sizes were measured microscopically in reflected light using a calibrated reticle. Modal analyses were made in reflected light at high magnification using an automated point counter. Mineral analyses were determined with the JEOL JXA-8200 electron microprobe at UCLA using natural and synthetic standards, an accelerating voltage of 15 keV, a 15 nA sample current, 20 s counting times, and ZAF corrections. Cobalt values in kamacite were corrected for the interference of the Fe-$K_\beta$ peak with the Co-$K_\alpha$ peak.

The modal abundance of metallic Fe-Ni and the mean olivine, low-Ca pyroxene, and kamacite compositions of Berduc indicate that the rock is an L-group chondrite. Berduc contains 8.1 wt% metallic Fe-Ni (Table 6) compared to 8.3 wt% in mean L-chondrite falls (Table 5 of Jarosewich 1990). Olivine (Fa 23.7 ± 0.5; n = 23), low-Ca pyroxene (Fs 20.3 ± 0.5, Wo 1.4 ± 0.2; n = 25), and kamacite (7.1 ± 0.8 mg/g Co; n = 7) in Berduc (Table 7) are within the compositional ranges characteristic of L chondrites (Fa 23.0–25.8; Fs 18.7–22.6; 7.0–9.5 mg/g Co; Rubin 1990; Gomes and Keil 1980).

Table 6. Modal abundances of major phases in Berduc.

| | Points | vol% | wt% |
|---|---|---|---|
| Silicate | 1998 | 91.8 | 85.9 |
| Metallic Fe-Ni | 79 | 3.6 | 8.1 |
| Troilite | 88 | 4.0 | 5.3 |
| Chromite | 12 | 0.6 | 0.7 |
| Total | 2177 | 100.0 | 100.0 |

Volume percent was converted into wt% using the following densities (g/cm$^3$): silicate (3.33), metallic Fe-Ni (7.9), troilite (4.67), chromite (4.7).

Berduc is highly recrystallized and contains poorly defined radial pyroxene (RP), porphyritic olivine (PO), porphyritic olivine-pyroxene (POP), and barred olivine (BO) chondrules that are well integrated into the matrix. Plagioclase grains typically exceed 50 μm in size, indicating that the rock is petrologic type 6. This is consistent with the relative compositional homogeneity of the olivine and low-Ca pyroxene.

Metallic Fe-Ni grains show no signs of alteration, consistent with weathering grade W0. Other phases in the rock include plagioclase (Ab 75.5 ± 1.6 Or 5.3 ± 0.7; n = 6), diopside (Fs 7.5 Wo 45; n = 2), chromite, troilite (essentially pure FeS), and rare metallic Cu (Tables 6 and 7). The rock has been moderately shocked, equivalent to shock stage S4 (Stöffler et al. 1991); many of the olivine grains contain planar fractures and exhibit weak mosaic extinction. Berduc contains 30–50 μm wide melt veins filled with glass, 0.2–0.8 μm size troilite grains, and lesser amounts of metallic Fe-Ni. Wider melt veins (50–150 μm thick) in the rock contain numerous 2–30 μm size round blebs of cellular troilite-metal intergrowths. Thin metal veins (3–5 μm thick) also occur. Some of these veins are connected to relatively coarse sheared metal grains.

Many of the troilite grains are polycrystalline (Fig. 5). Veins of troilite (100 μm long, 0.2 μm thick) traverse some of the mafic silicate grains. A few large metallic Fe-Ni grains contain irregular 2–8 μm size grains of troilite. One 7 μm size metallic-Cu grain was observed; it occurs within an opaque assemblage at the interface between troilite and metallic Fe-Ni. Chromite occurs as extensively fractured isolated grains, as 1 μm thick, 35 μm long veinlets that transect olivine grains (Fig. 6), and in ~50 μm size chromite-plagioclase assemblages (e.g., Rubin 2003). Many of the plagioclase grains are irregular in shape and appear to have flowed and coalesced. Shock melting of the plagioclase and concomitant volatilization of Na could account for the relatively low Ab contents (75.5 mol%) in Berduc

Table 7. Mineral compositions (wt%) in Berduc.

| | Olivine | Low-Ca pyx | Diopside | Plagioclase | Chromite | | Kamacite |
|---|---|---|---|---|---|---|---|
| No. grains | 23 | 25 | 2 | 8 | 10 | No. grains | 7 |
| $SiO_2$ | 38.5 ± 0.4 | 56.1 ± 0.4 | 54.4 | 65.8 ± 0.3 | < 0.04 | Cr | < 0.04 |
| $TiO_2$ | < 0.04 | 0.18 ± 0.04 | 0.49 | 0.04 ± 0.01 | 2.4 ± 0.3 | Fe | 92.6 ± 0.8 |
| $Al_2O_3$ | < 0.04 | 0.15 ± 0.03 | 0.53 | 22.5 ± 0.6 | 6.6 ± 0.2 | Co | 7.1 ± 0.8 |
| $Cr_2O_3$ | < 0.04 | 0.10 ± 0.07 | 0.81 | < 0.04 | 56.7 ± 0.4 | Ni | 6.3 ± 0.5 |
| FeO | 22.3 ± 0.5 | 13.8 ± 0.4 | 4.7 | 0.27 ± 0.6 | 31.5 ± 0.3 | Total | 99.6 |
| MnO | 0.46 ± 0.04 | 0.48 ± 0.03 | 0.23 | < 0.04 | 0.84 ± 0.07 | | |
| MgO | 40.2 ± 0.3 | 29.9 ± 0.2 | 16.9 | < 0.04 | 2.4 ± 0.3 | | |
| CaO | < 0.04 | 0.76 ± 0.12 | 22.1 | 2.2 ± 0.1 | < 0.04 | | |
| $Na_2O$ | < 0.04 | < 0.04 | 0.62 | 9.4 ± 0.5 | < 0.04 | | |
| $K_2O$ | < 0.04 | < 0.04 | < 0.04 | 1.0 ± 0.1 | < 0.04 | | |
| Total | 101.5 | 101.5 | 100.8 | 101.2 | 100.4 | | |
| Endmember (mol%) | Fa 23.7 ± 0.5 | Fs 20.3 ± 0.5<br>Wo 1.4 ± 0.2 | Fs 7.5<br>Wo 45 | Ab 75.5 ± 1.6<br>Or 5.3 ± 0.7 | | | |

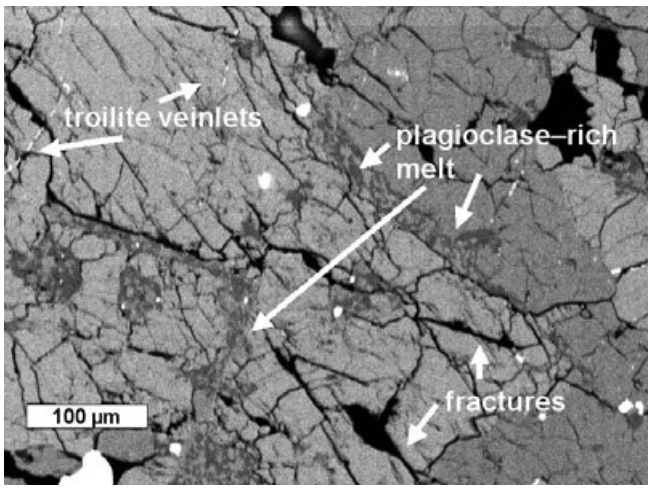


Fig. 6. Thin troilite veinlets and anastomosing plagioclase-rich melt veins occur throughout Berduc. Also present are numerous fractures in the mafic silicate grains.

compared with mean L-chondrite plagioclase (Ab 84.2 mol%; Van Schmus and Ribbe 1968).

## BULK CHEMISTRY

Abundances of 36 chemical elements were determined in two different samples of about 2.2 g from the interior of two Berduc meteorite specimens following the procedures described in Llorca et al. (2007). Briefly, analyses of trace elements were performed by means of inductively coupled plasma–mass spectrometry (ICP-MS), whereas major and minor elements were analyzed by inductively coupled plasma–optical emission spectroscopy (ICP-OES). Samples were ground to powder using an agate mortar and pestle and dried at 378 K. Two separate methods were used for sample preparation. The first method consisted of an acid digestion treatment of samples in a sealed Teflon reactor at 363 K (four replicates). The second method consisted of an alkaline fusion in a zirconium crucible at 723 K (two replicates). Some elements were analyzed by both methods and the results were in agreement. Thus, in addition to routine analysis control with reference materials, the accuracy of the procedures was demonstrated by the replicate analyses. Table 8 shows the elemental composition of the Berduc meteorite. Mean values and mean uncertainties are listed, and the resulting bulk composition is compared with the average composition of L6 chondrites (Kallemeyn et al. 1989; Friedrich et al. 2003). The content of Fe (22.0%) and the values of Mg/Si = 0.88, Al/Si = 0.06, and Fe/Si = 1.18 closely match the values of L-group chondrites. For most elements, the measured abundances are within the range observed for L6 chondrites, and values within 20% of the average are found. Elemental abundances are consistent with the interpretation of Berduc being an L6 chondrite of rather normal chemistry.

## MAGNETIC PROPERTIES, DENSITY, AND POROSITY

For magnetic measurements, two samples of about 2.2 g of Berduc were taken from the interior of separate pieces of the meteorite. Hysteresis loops were run on each sample and the saturation magnetization, $J_S$, the remanent saturation magnetization, $J_{RS}$, and the coercive force, $H_C$, were determined as explained elsewhere (Llorca et al. 2007). Magnetic susceptibility measurements were made at a low field (0.5 mT). The hysteresis loops and the magnetic data for both Berduc specimens were very similar and indicate the magnetic

Table 8. Elemental abundances in the Berduc meteorite.

| Element | Unit | Sample preparation | Method | Berduc | Ratio to L6 chondrites[a] |
|---|---|---|---|---|---|
| Li | μg/g | a.d. | ICP-MS | 1.8 ± 0.3 | 0.99 |
| Na | mg/g | a.d. | ICP-OES | 6.9 ± 0.1 | 0.98 |
| Mg | mg/g | a.d. | ICP-OES | 161.3 ± 4.8 | 1.10 |
| | | a.f. | ICP-OES | 165.1 ± 5.0 | |
| Al | mg/g | a.d. | ICP-OES | 12.3 ± 0.3 | 0.99 |
| | | a.f. | ICP-OES | 11.8 ± 0.3 | |
| Si | mg/g | a.f. | ICP-OES | 185.6 ± 5.1 | 0.99 |
| P | μg/g | a.d. | ICP-OES | 1002 ± 25 | 1.05 |
| S | mg/g | a.d. | ICP-OES | 23.0 ± 0.7 | 1.04 |
| K | μg/g | a.d. | ICP-OES | 778 ± 110 | 0.92 |
| Ca | mg/g | a.d. | ICP-OES | 14.1 ± 0.3 | 1.05 |
| | | a.f. | ICP-OES | 13.2 ± 0.6 | |
| Sc | μg/g | a.d. | ICP-MS | 8.7 ± 0.3 | 1.03 |
| Ti | μg/g | a.d. | ICP-OES | 640 ± 7.1 | 0.98 |
| Cr | mg/g | a.f. | ICP-OES | 3.5 ± 0.1 | 0.92 |
| Mn | mg/g | a.d. | ICP-OES | 2.6 ± 0.1 | 1.01 |
| Fe | mg/g | a.d. | ICP-OES | 222.6 ± 4.2 | 1.01 |
| | | a.f. | ICP-OES | 217.0 ± 4.3 | |
| Co | μg/g | a.d. | ICP-OES | 584 ± 17 | 1.00 |
| Ni | mg/g | a.d. | ICP-OES | 13.2 ± 0.2 | 1.08 |
| Cu | μg/g | a.d. | ICP-MS | 99 ± 0.6 | 0.95 |
| Zn | μg/g | a.d. | ICP-MS | 57 ± 0.7 | 1.04 |
| Ga | μg/g | a.d. | ICP-MS | 5.7 ± 0.9 | 1.03 |
| Ge | μg/g | a.d. | ICP-MS | 7.9 ± 0.9 | 0.88 |
| Rb | μg/g | a.d. | ICP-MS | 3.02 ± 0.03 | 1.08 |
| Sr | μg/g | a.d. | ICP-MS | 11.7 ± 0.1 | 1.17 |
| Y | μg/g | a.d. | ICP-MS | 2.2 ± 0.04 | 1.01 |
| | | a.f. | ICP-MS | 2.6 ± 0.1 | |
| Zr | μg/g | a.d. | ICP-MS | 7.3 ± 0.1 | 0.94 |
| Mo | μg/g | a.d. | ICP-MS | 2.3 ± 0.1 | 1.12 |
| Ru | μg/g | a.d. | ICP-MS | 1.27 ± 0.02 | 1.01 |
| Pd | μg/g | a.d. | ICP-MS | 0.66 ± 0.02 | 1.05 |
| Te | μg/g | a.d. | ICP-MS | 0.45 ± 0.02 | 1.03 |
| Ba | μg/g | a.d. | ICP-MS | 3.7 ± 0.1 | 0.96 |
| Ce | μg/g | a.d. | ICP-MS | 0.9 ± 0.1 | 1.01 |
| Eu | μg/g | a.d. | ICP-MS | 0.09 ± 0.01 | 1.13 |
| Os | μg/g | a.d. | ICP-MS | 0.5 ± 0.1 | 0.91 |
| Ir | μg/g | a.d. | ICP-MS | 0.60 ± 0.02 | 1.14 |
| Pt | μg/g | a.d. | ICP-MS | 1.1 ± 0.1 | 1.05 |
| Th | μg/g | a.d. | ICP-MS | 0.05 ± 0.01 | 1.19 |
| U | μg/g | a.d. | ICP-MS | 0.02 ± 0.00 | 1.18 |

a.d., acid digestion; a.f., alkaline fusion.
[a]Reference values taken from Friedrich et al. (2003) and Kallemeyn et al. (1989).

homogeneity of this meteorite (as is the case for most ordinary chondrites; Gattacceca et al. 2003). Specific magnetic susceptibility, $\chi$, gave a log $\chi$ of 4.81 ± 0.05 (in $10^{-9}$ $m^3/kg$), typical of other L chondrite falls, 4.87 ± 0.10 (Rochette et al. 2003; Consolmagno et al. 2006) and 4.87 ± 0.08 (Smith et al. 2006). Similarly, the log $J_S$ and log $J_{RS}$ recorded values of 1.35 ± 0.05 and 8.2 ± 0.1 (in $10^{-3}$ $Am^2/kg$), respectively, are in the range of other L chondrites (Sugiura and Strangway 1987); the value of the coercive force of 13.5 ± 0.5 (in $10^{-4}$ T) was also in the L-chondrite range. In summary, the Berduc meteorite has bulk magnetic properties in good agreement with other studied L6 chondrites.

Magnetic susceptibility and grain density ($\rho_g$, density that excludes pores and voids) are commonly correlated for meteorite falls because both are intensive variables that vary with iron content (Britt and Consolmagno 2003; Consolmagno et al. 2006). The

Table 9. Measured activities of short-lived radionuclides in Berduc.

| | Current activity (September 2008) | | Activity at the time of fall | |
|---|---|---|---|---|
| Isotope | (mBq/kg) | (dpm/kg) | (mBq/kg) | (dpm/kg) |
| $^{238}$U | 82.53 ± 39.66 | 4.95 ± 2.38 | 82.53 ± 39.66 | 4.95 ± 2.38 |
| $^{226}$Ra | 940.70 ± 576.80 | 56.44 ± 34.61 | 940.70 ± 576.80 | 56.44 ± 34.61 |
| $^{232}$Th | 78.30 ± 22.18 | 4.70 ± 1.33 | 78.30 ± 22.18 | 4.70 ± 1.33 |
| $^{40}$K | 23017 ± 1291 | 1381.02 ± 77.46 | 23017 ± 1291 | 1381.02 ± 77.46 |
| $^{60}$Co | 406.65 ± 40.65 | 24.40 ± 2.44 | 406.65 ± 40.65 | 24.40 ± 2.44 |
| $^{137}$Cs | < 49.40 | < 2.96 | < 49.40 | < 2.96 |
| $^{26}$Al | 646.77 ± 75.27 | 38.81 ± 4.52 | 646.77 ± 75.27 | 38.81 ± 4.52 |
| $^{22}$Na | 997.13 ± 84.67 | 59.83 ± 5.08 | 1112.50 ± 94.47 | 66.75 ± 5.67 |
| $^{57}$Co | 172.25 ± 23.49 | 10.33 ± 1.41 | 252.65 ± 34.45 | 15.16 ± 2.07 |
| $^{51}$Cr | < 58.00 | < 3.48 | < 2475.00 | < 148.50 |
| $^{7}$Be | < 384.59 | 23.08 ± 0.00 | < 2705.00 | < 162.30 |
| $^{58}$Co | 78.26 ± 27.69 | 4.70 ± 1.66 | 339.90 ± 120.26 | 20.39 ± 7.22 |
| $^{54}$Mn | 1518.13 ± 90.94 | 91.09 ± 5.46 | 2118.00 ± 126.87 | 127.08 ± 7.61 |
| $^{56}$Co | < 38.93 | 2.34 ± 0.00 | < 145.50 | < 8.73 |
| $^{46}$Sc | 52.36 ± 24.16 | 3.14 ± 1.45 | 180.80 ± 83.42 | 10.85 ± 5.01 |
| $^{48}$V | 67.01 ± 23.89 | < 4.02 ± 1.43 | 44500 ± 15865 | 2670 ± 952 |
| $^{52}$Mn | < 23.12 | < 1.39 | – | |
| Berduc Fall April 7, 2008 | $^{22}$Na/$^{26}$Al | | $^{22}$Na/$^{26}$Al | |
| Ge analysis Sept. 3, 2008–Sept. 10, 2008 | | 1.54 | | 1.72 |

grain density of the Berduc meteorite determined with a helium pycnometer was 3.62 ± 0.05 g/cm$^3$. The values of magnetic susceptibility and grain density of Berduc plot well within the L-chondrite group in a $\chi$ versus $\rho_g$ graph for meteorite falls (Consolmagno et al. 2006). From the grain density and the bulk density value of 3.54 ± 0.05 g/cm$^3$, the porosity of Berduc is calculated to be 2.2%.

## COSMOGENIC RADIONUCLIDES

Gamma spectroscopy performed in September 2008 with the ultralow noise germanium detector located in the road tunnel of "La Vue-des-Alpes," Switzerland, 600 m water-equivalent underground, showed the presence of the following short-lived radionuclides: $^{48}$V, $^{46}$Sc, $^{54}$Mn, $^{58}$Co, $^{57}$Co, $^{22}$Na, $^{60}$Co, $^{26}$Al. Recalculated to April 7, 2008, $^{22}$Na was 66.8 ± 5.7 dpm/kg and $^{26}$Al 38.8 ± 4.5 dpm/kg. The presence of short-lived isotopes and the $^{22}$Na/$^{26}$Al activity ratio of 1.7 calculated for the time of fall are consistent with a fall in April 2008 (see Table 9). We were trying to find additional evidence for the pre-atmospheric size of the meteoroid, but an activity of 39 dpm/kg does not provide a lot of information about this parameter. By comparing the Berduc data with the graph on the production of $^{26}$Al in chondrites (Leya et al. 2000), we conclude that the studied sample comes from the near surface of the meteorite, from an approximate depth of 10 cm.

## CONCLUSIONS

A meter-size meteoroid produced a bright bolide that was observed over Argentina and Uruguay on April 7, 2008 at 01 h 02 min 28 s ± 1 s UTC. The event was also recorded by an infrasound array in Paraguay. This bolide produced a meteorite fall in a remote area called Colonia Berduc, near the Uruguay border. A few days after the fall, several members of Asociación Entrerriana de Astronomía recovered the first meteorites that were studied by our team. The Berduc meteorite is characterized as an L6 ordinary chondrite. Olivine, low-Ca pyroxene, and kamacite values are within the compositional ranges characteristic of L chondrites. Bulk chemistry also reveals a close match to this chondrite group. After interviewing about 30 casual eyewitnesses, consistent reports were obtained from six locations. These data, together with the strewn field and infrasound constraints, allowed the determination with moderate accuracy of the atmospheric trajectory, radiant, and range of orbital elements of the progenitor meteoroid. Some assumptions on the bolide pre-atmospheric velocity suggest an origin in the main asteroid belt as in the case of the nine previous meteorites with known orbital elements (Trigo-Rodríguez et al. 2006).

Note added in proof. At the time of publication of this paper the 10th meteorite with accurate orbit has been obtained. See Bland et al. (2009) for additional details.

*Acknowledgments*—We would like to express our gratitude to Dr. María Eugenia Varela (CASLEO) for the information provided on the Berduc samples preserved in Argentina. We also thank the search tasks promoted by the members of Asociación Entrerriana de Astronomía: Alberto Anunziato, Gustavo Blettler, Milton N. Blumhagen, Marcelo R. Bonnin, Mariano A. Peter, Jose Pasgal, Gabriela Pretto, Juan P. Sotera, and Luis Trumper. The DAFC (Uruguay) team that visited the area was made up, among others, by Leda Sánchez, Andrea Sánchez, Sebastián Bruzzone, and Julia Venturini. Their contribution was essential for the collection of the witnesses' accounts and their collaboration is greatly appreciated. We also thank the eyewitnesses who provided information on the bolide trajectory: M. Balsamo, M. Barga, M. Barrios, R. Belotti, A. Berreta, V. Cabrera, F. Calleros, J. C. Chacon, V. Cosseres, G. Cremaschi, J. DaCunha, I. Duque, N. Duque, N. Flores, F. Frascheri, N. Golden, A. Gutiérrez, N. Haget, M. Inda, M. Medina, D. Méndez, M. Morahan, E. Neris, L. Pacheco, E. Perez, D. Reyes, L. Reyes, J. Ribero, F. Ruiz Díaz, M. Ruíz Arzadum, V. Saavedra, V. Santellán, C. Teixeira, G. Vignolo, H. Weber, L. Wittman, and especially the students of Paysandu's High School. Óscar A. Turone also provided valuable data on the area, and recovered one of the meteorite samples that we studied. We are grateful to the infrasound preliminary analysis performed by Peter Brown (University of Western Ontario, Canada). J. M. T. R. also thanks CSIC for a JAE-Doc research contract, and acknowledges funding from AYA2008-01839/ESP. W. N. E. thanks the British Atmospheric Data Center (BADC) for access to weather data from the UKMO assimilated data set. This work was also supported in part by NASA Cosmochemistry grant NNG06GF95G (A. E. R.).

*Editorial Handling*—Dr. Ellen Beth Clark

## REFERENCES

Arrowsmith S. J., Drob D. P., Hedlin M. A. H., and Edwards W. 2007. A joint seismic and acoustic study of the Washington state bolide: Observations and modeling. *Journal of Geophysical Research* 112, doi:10.1029/2006JD008001.

Bland P. A., Spurny P., Towner M. C., Bevan A. W. R., Singleton A. T., Bottke W. F., Jr, Greenwood R. C., Chesley S. R., Shrbeny L., Borovicka J., Ceplecha Z., McClafferty T. P., Vaughan D., Benedix G. K., Deacon G., Howard K. T., Franchi I. A., and Hough R. M. 2009. An anomalous basaltic meteorite from the innermost Main Belt. *Science* 325:1525–1527.

Britt D. T. and Consolmagno G. J. 2003. Stony meteorite porosities and densities: A review of the data through 2001. *Meteoritics & Planetary Science* 38:1161–1180.

Brown P., Spalding R. E., ReVelle D. O., Tagliaferri E., and Worden S. P. 2002. The flux of small near-Earth objects colliding with the Earth. *Nature* 420:294–296.

Ceplecha Z. 1987. Geometric, dynamic, orbital and photometric data on meteoroids from photographic fireball networks. *Bulletin of the Astronomical Institute of Czechoslovakia* 38:211–222.

Consolmagno G. J., Macke R. J., Rochette P., Britt D. T., and Gattacceca J. 2006. Density, magnetic susceptibility, and the characterization of ordinary chondrite falls and showers. *Meteoritics & Planetary Science* 41:331–342.

Docobo J. A., Trigo-Rodríguez J. M., Borovicka J., Tamazian V. S., Fernandes V. A., and Llorca J. 2008. March 1, 2005 daylight fireball over Galicia (NW of Spain) and Minho (N Portugal). *Earth Moon and Planets* 102:537–542.

Edwards W. N., Brown P. G., and ReVelle D. O. 2006. Estimates of meteoroid kinetic energies from observations of infrasonic airwaves. *Journal of Atmospheric and Solar-Terrestrial Physics* 68:1136–1160.

Friedrich J. M., Wang M. S., and Lipschutz M. E. 2003. Chemical studies of L chondrites. V: Compositional patterns for 49 trace elements in 14 L4–6 and 7 LL4–6 falls. *Geochimica et Cosmochimica Acta* 67:2467–2479.

Gattacceca J., Rochette P., and Bourot-Denise M. 2003. Magnetic properties of a freshly fallen LL ordinary chondrite: The Bensour meteorite. *Physics of the Earth and Planetary Interiors* 140:343–358.

Gomes C. B. and Keil K. 1980. *Brazilian stone meteorites*. Albuquerque, NM: The University of New Mexico Press. 161 p.

Jarosewich E. 1990. Chemical analyses of meteorites: A compilation of stony and iron meteorite analyses. *Meteoritics* 25:323–337.

Kallemeyn G. W., Rubin A. E., Wang D., and Wasson T. W. 1989. Ordinary chondrites: Bulk compositions, classification, lithophile-element fractionations, and composition-petrographic type relationships. *Geochimica et Cosmochimica Acta* 53:2747–2767.

Leya I., Lange H.-J., Neumann S., Wieler R., and Michel R. 2000. The production of cosmogenic nuclides in stony meteoroids by galactic cosmic-ray particles. *Meteoritics & Planetary Science* 35:259–286.

Llorca J., Trigo-Rodríguez J. M., Ortiz J. L., Docobo J. A., Garcia-Guinea J., Castro-Tirado A. J., Rubin A. E., Eugster O., Edwards W., Laubenstein M., and Casanova I. 2005. The Villalbeto de la Peña meteorite fall: I. Fireball energy, meteorite recovery, strewn field and petrography. *Meteoritics & Planetary Science* 40:795–804.

Llorca J., Gich M., and Molins E. 2007. The Villalbeto de la Peña meteorite fall: III. Bulk chemistry, porosity, magnetic properties, 57Fe Mössbauer spectroscopy, and Raman spectroscopy. *Meteoritics & Planetary Science* 42:177–182.

Rochette P., Sagnotti L., Bourot-Denise M., Consolmagno G., Folco L., Gattacceca J., Osete M. L., and Pesonen L. 2003. Magnetic classification of stony meteorites. 1. Ordinary chondrites. *Meteoritics & Planetary Science* 38:251–268.

Rubin A. E. 1990. Kamacite and olivine in ordinary chondrites: Intergroup and intragroup relationships. *Geochimica et Cosmochimica Acta* 54:1217–1232.

Rubin A. E. 2003. Chromite-plagioclase assemblages as a new shock indicator; implications for the shock and thermal histories of ordinary chondrites. *Geochimica et Cosmochimica Acta* 67:2695–2709.

Smith D. L., Ernst R. E., Samson C., and Herd R. 2006. Stony meteorite characterization by non-destructive measurement of magnetic properties. *Meteoritics & Planetary Science* 41:355–373.

Stöffler D., Keil K., and Scott E. R. D. 1991. Shock metamorphism of ordinary chondrites. *Geochimica et Cosmochimica Acta* 55:3845–3867.

Sugiura N. and Strangway D. W. 1987. Magnetic studies of meteorites. In *Meteorites and the early solar system*, edited by Kerridge J. and Matthews M. Tucson, AZ: The University of Arizona Press. pp. 595–615.

Swinbank R. and O'Neill A. A. 1994. Stratosphere–troposphere data assimilation system. *Monthly Weather Review* 122:686–702.

Trigo-Rodríguez J. M., Borovička J., Spurný P., Ortiz J. L., Docobo J. A., Castro-Tirado A. J., and Llorca J. 2006. The Villalbeto de la Peña meteorite fall: II. Determination of the atmospheric trajectory and orbit. *Meteoritics & Planetary Science* 41:505–517.

Trigo-Rodríguez J. M., Llorca J., Rubin A. E., Grossman J. N., Sears D. W. G., Naranjo M., Bretzius S., Tapia M., and Guarín Sepúlveda M. H. 2009. The Cali meteorite fall: A new H/L ordinary chondrite. *Meteoritics & Planetary Science* 44:211–220.

Van Schmus W. R. and Ribbe P. H. 1968. The composition and structural state of feldspar from chondritic meteorites. *Geochimica et Cosmochimica Acta* 32:1327–1342.

Weisberg M. K., Smith C., Benedix G., Herd C. D. K., Righter K., Haack H, Yamaguchi A., Chennaoui Houdjehane H., and Grossman J. N. 2009. The Meteoritical Bulletin, No. 96. *Meteoritics & Planetary Science* 44:1355–1397.